Stress-induced relaxation mechanisms in single-crystalline titanomagnetites

2003 J. Phys.: Condens. Matter 15 7029

(http://iopscience.iop.org/0953-8984/15/41/011)

INSTITUTE OF PHYSICS PUBLISHING JOURNAL OF PHYSICS: CONDENSED MATTER

J. Phys.: Condens. Matter **15** (2003) 7029–7045 PII: S0953-8984(03)66573-2

Stress-induced relaxation mechanisms in single-crystalline titanomagnetites

F Walz[1], V A M Brabers[2], J H V J Brabers[3] and H Kronmüller[1]

[1] Max-Planck-Institut für Metallforschung, Stuttgart, Germany
[2] Department of Physics, Eindhoven University of Technology, Eindhoven, The Netherlands
[3] Philips Centre for Industrial Technology, Eindhoven, The Netherlands

Received 29 July 2003
Published 3 October 2003
Online at stacks.iop.org/JPhysCM/15/7029

Abstract

The effect of titanium (Ti^{4+}) substitution on slightly oxidized magnetite single crystals, $Fe_{3-x}Ti_xO_{4+\delta}$—with $0.1 \leqslant x \leqslant 1.0$ and $\delta \leqslant 0.005$—is studied by means of magnetic after-effect (MAE) spectroscopy in the temperature range $4\ \mathrm{K} < T \leqslant 500\ \mathrm{K}$. The MAE spectra corresponding to these, relatively high, substitution rates are characterized by the following items: (i) suppression of low-temperature ($4\ \mathrm{K} < T < 35\ \mathrm{K}$) electron ($e^-$)-tunnelling; (ii) severely damaged variable-range e^--hopping ($50\ \mathrm{K} < T < 125\ \mathrm{K}$), culminating in a pronounced 'negative' (sign-reversed) Debye-type peak near 65 K; (iii) the occurrence of a remarkable MAE near 210 K, being identified as resulting from reorientations of intrinsic interstitials which had formed under the action of Ti^{4+}-induced lattice distortions; (iv) the nearly complete suppression of all 'type III' related, vacancy-mediated relaxations near 300 K; (v) the occurrence of a huge, 'type II' relaxation maximum being situated initially ($x \simeq 0.1$) near 480 K and—proportionally with *increasing* doping—shifted to *lower* temperatures, reaching $T_{max} \simeq 380\ \mathrm{K}$ for $x = 0.6$. These processes are shown to interfere with internal stresses induced into the orthogonal (B) sublattice upon Ti-doping due to the transformation of Fe^{3+} into more extended Fe^{2+} ions which have a greater volume. This stress induction is found to reach its maximum near $x = 0.2$; its decay on further doping is explained by the beginning of a re-substitution of Fe^{2+} ions from B- onto A-sites of the tetrahedral sublattice.

1. Introduction

In previous studies we investigated the influence of Ti-doping ($0.01 \leqslant x \leqslant 0.4$) on the magnetic after-effect (MAE) spectra of *polycrystalline* magnetite (Fe_3O_4) over a wide temperature range ($4\ \mathrm{K} < T < 450\ \mathrm{K}$) and found it to specifically modify the inherent relaxation mechanisms and to induce new, doping-dependent processes [1, 2]. These interesting results suggested continuing with corresponding studies on *single-crystalline*, Ti-doped magnetite ($Fe_{3-x}Ti_xO_4$) within the extended parameter ranges of $0.0001 \leqslant x \leqslant 1.0$ and

$4\ \mathrm{K} < T \leqslant 500\ \mathrm{K}$ in order to obtain more detailed information on the underlying atomistic mechanisms.

As pointed out in a recent review [3], the MAE—especially in magnetite and related ferrites—is a most efficient tool for the detection of any type of time-dependent lattice interaction with the spontaneous magnetization inside domain walls[4]. Generally, MAEs in stoichiometric Fe_3O_4 originate from a combined local charge and anisotropy transport between adjacent divalent and trivalent Fe ions, resulting in an exchange of their lattice positions. Interestingly, two different mechanisms for such valency exchange are feasible in magnetite, namely either (1) *electronic*- or (2) vacancy-mediated *ionic* charge transfer

$$\mathrm{Fe}_1^{2+} + \mathrm{Fe}_2^{3+} \quad \rightleftarrows \quad \mathrm{Fe}_1^{3+} + \mathrm{Fe}_2^{2+} \tag{1}$$

$$\mathrm{Fe}_1^{2+} + \mathrm{Fe}_2^{3+} + \square_3 \quad \rightleftarrows \quad \square_1 + \mathrm{Fe}_1^{3+} + \mathrm{Fe}_2^{2+} \tag{2a}$$

$$\mathrm{Fe}_1^{2+} + \mathrm{Fe}_2^{3+} + \square_3 \quad \rightleftarrows \quad \mathrm{Fe}_1^{3+} + \square_2 + \mathrm{Fe}_3^{2+} \tag{2b}$$

which, indeed, are both found to contribute specific relaxation processes to the MAE spectra[5]. As has been thoroughly investigated and pointed out in a recent review [3], the electronically induced processes (1) are fully developed only in stoichiometric, defect-free Fe_3O_4—preferentially of single crystalline structure—where they are confined to the low-temperature phase ($4\ \mathrm{K} < T < 125\ \mathrm{K}$), being characterized by long-range electronic ordering. Only under these conditions, electron transfer according to (1)—achieved by means of either incoherent tunnelling ($4\ \mathrm{K} < T < 35\ \mathrm{K}$) or variable range hopping ($50\ \mathrm{K} < T < T_V \simeq 125\ \mathrm{K}$)—is able to induce pronounced MAE spectra. At $T_V \simeq 125$ K, stoichiometric Fe_3O_4 undergoes a first-order crystallographic phase transition, named after Verwey [3], which is characterized by the breakdown of low-temperature electronic order, thus inducing a spontaneous rise of the electric conductivity (by about a factor 100) and a corresponding acceleration of the electronic transfer rates out of the detection range of the MAE spectroscopy ($\tau < 1$ s), cf section 2.2.

Within the high-temperature range ($T_V < T \leqslant 500$ K), in *nonstoichiometric* crystals a second type of charge transfer processes—described in terms of relations (2)—is feasible, originating from thermally activated *B-site vacancy*-mediated diffusion of intrinsic and/or substituted foreign ions. Indeed, most of the MAE spectra occurring above T_V in imperfect magnetite and related compounds are induced from ionic processes following such type-(2) mechanisms [8–12], cf figure 6(b).

As is known from numerous experiments on differently impurity-charged[6] magnetite poly- and single crystals, the electronic tunnelling processes ($4\ \mathrm{K} < T < 35\ \mathrm{K}$) are strongly affected by the smallest deviations from stoichiometry, and at doping rates of $x \leqslant 0.05$ are nearly completely suppressed [12]. On the other hand, variable-range electron hopping—occurring typically in the temperature interval $50\ \mathrm{K} < T < 125\ \mathrm{K}$—proves to be more resistant against

[4] This statement, naturally, holds as well for all other ferrimagnetic and ferromagnetic [4] materials and, moreover, has been found to be true also for ferroelectric compounds [5] —with respect to interactions of corresponding defects with ferroelectric domain walls.

[5] The clue to correspondingly induced MAE mechanisms consists of the different orbital moments of the Fe^{3+} and Fe^{2+} ions—associated with their groundstates of, respectively, $d^5{:}^6S_{5/2}$ and $d^6{:}^5D_4$—which preserve, qualitatively, their free ion items also in the spinel lattice, namely zero momentum (Fe^{3+}) and non-zero (lattice-quenched) residual momentum (Fe^{2+}). Alignment of the corresponding Fe^{2+} anisotropy axes relative to the spontaneous intra-domain wall magnetization—after preceding electronically (equation (1)) or ionically (equation (2)) induced anisotropy transport—leads to a lowering of the interaction potential and hence reduction of the domain wall mobility, thereby giving rise to the macroscopically observable MAEs [6, 7]. Equations (2*a*) and (2*b*) describe the case where an Fe^{2+} ion is jumping (1) either directly or (2) after capturing of a thermally dissociated electron—with a correspondingly enhanced activation enthalpy—into a neighbouring B-site vacancy (figure 6(b)), cf [8–11].

[6] Corresponding observations have been made after doping with Ba^{2+}, Mn^{2+}, Ni^{2+}, Co^{2+}, Mg^{2+}, Zn^{2+}, Ga^{3+}, Ti^{4+} and in the presence of B-site (octahedral) vacancies [8, 9], as described and referred to in [3, 8–12].

various types of lattice perturbations, thus remaining observable up to higher doping rates of $x(Ti^{4+}) \leqslant 0.3$—though with considerably modified and mutilated shape as compared to stoichiometric crystals [1–3, 10–12], cf figures 1 to 3(a).

As regards the literature on titanomagnetites, most of recent work is concerned with exploring the influence of relatively *weak* Ti-doping ($x < 0.05$) on the *electronic* processes of the low-temperature phase ($T \leqslant T_V \simeq 125$ K)—thereby using a variety of techniques such as electric conductivity [13, 14], thermoelectricity [13], specific heat [15], various magnetic [16–18] and other methods, as summarized in [3, 19, 20]—in order to clarify the conduction mechanisms in perfectly stoichiometric single-crystalline magnetite. The contributions of MAE studies to the solution of this problem [1–12] have been summarized in a recent review on the Verwey transition in magnetite [3].

In contrast to this general trend, our present report is mainly concerned with higher charged compounds—$Fe_{3-x}Ti_xO_{4+\delta}$; $0.1 \leqslant x \leqslant 1.0$ and $\delta \simeq 0.005$ [21] —which, so far, have been less systematically investigated with the MAE. Moreover, in order to complete previous MAE studies [1, 2, 17, 18, 22–24] which were performed on *polycrystalline* materials, we present here the first consistent data set obtained on *single-crystals*.

As expected from our above argument, the MAE spectra in these compounds are found to be dominated by ionically induced reorientation-type processes, occurring at temperatures above 150 K. Interestingly, of the electronic low-temperature (50 K $< T <$ 125 K) processes, a drastically modified residuum of small-polaron hopping survives up to $x \leqslant 0.3$, whereas the lower tunnelling processes (4 K $< T <$ 35 K) are completely suppressed, cf figures 1 to 3(a).

Two effects are regarded to be of major significance concerning the underlying relaxation mechanisms of our present MAE spectra: (i) the appearance of a *sign-reversed* (negative) peak near 65 K, i.e., a doping-induced modification of small-polaron hopping which—to our knowledge—has not been observed as yet with such clarity in any other magnetite-based compound, and (ii) a considerable, doping-proportional shift of the Ti-induced peak II from *higher* ($T \simeq 480$ K for $x \leqslant 0.1$) to *lower* temperatures ($T \simeq 380$ K for $x = 0.6$), which in previously investigated *polycrystals* could not be resolved in comparable detail [1, 2, 23].

2. Experimental details

2.1. Specimens

The $Fe_{3-x}Ti_xO_4$ single crystals studied in our experiments were grown, using a floating zone technique, in form of rods with their axis oriented along ⟨110⟩ and with typical dimensions of length and diameter, respectively, of 3 and 0.5 cm. After the crystallization process they were annealed at 1200 °C in H_2/H_2O or CO/CO_2 atmospheres in order to improve their mechanical quality; thereby B-site vacancies, corresponding to an oxygen excess of $\delta \leqslant 0.005$, were introduced into the $Fe_{3-x}Ti_xO_{4+\delta}$ compounds [21, 25]. For MAE measurements these rods were cut by spark erosion into prisms with dimensions 20 mm × 1.4 mm × 1.4 mm.

2.2. Measuring technique

The isochronal MAE spectra, as presented in the following, result from isothermal relaxations of the initial reluctivity $r(t, T)$—i.e., the reciprocal initial susceptibility $r(t, T) = 1/\chi(t, T)$—as measured, at narrowly spaced temperatures, within extended intervals of typically 4 K $<$ $T <$ 500 K by means of an automated LC-oscillator technique in the 1 kHz range [26]. Out of these isothermals—whose measurements were started at $t_1 = 1$ s after sample demagnetization

and continued over the interval 2 s $\leqslant t_2 \leqslant$ 180 s—isochronals are constructed in the following way:

$$\frac{\Delta r}{r_1} = \frac{\Delta r(t_1, t_2, T)}{r(t_1, T)} = \frac{r(t_2, T) - r(t_1, T)}{r(t_1, T)}. \tag{3}$$

This type of data presentation has the inherent advantage of immediately separating multiprocess relaxations into their different constituents, all of which contributing individually—i.e., in form of peaks, plateaus, etc—to the observed MAE spectrum [4, 27].

2.3. Numerical analysis

As described in more detail elsewhere [4, 27, 28], MAEs, occurring after sample demagnetization at constant temperature T, may be generally described by the relation

$$r(t, T) = r_0(T) + \Delta r_s G(t, T), \tag{4}$$

where r_0 is the temperature-dependent initial reluctivity (at $t = 0$ s), Δr_s the maximum relaxation amplitude, attained in the limit $t \to \infty$, and $G(t, T)$ the generalized relaxation function. In the elementary case of only one single, thermally activated Debye process, $G(t)$ may be expressed by the simple exponential

$$G(t, T) = 1 - \exp(-t/\tau), \tag{5}$$

with τ the relaxation time of the process:

$$\tau = \tau_0 \exp\left(\frac{Q}{kT}\right), \tag{6}$$

as expressed in terms of the pre-exponential factor τ_0, the asymptotic particle jump time for $T \to \infty$ (cf table 1), the activation enthalpy Q (assumed to be constant throughout the temperature range of each single process) and the Boltzmann constant k. With respect to the experimental situation, it is more realistic to regard a given relaxation process as resulting from a continuous superposition of elementary relaxation functions of type (5), all of them obeying a characteristic distribution of the relaxation times $p(\tau)$ or, via equation (6), of the activation enthalpies, $p^*(Q)$, within a certain interval. In praxis, the rectangular box-type distribution extending with constant amplitude, $p(\tau)$, over an interval $\tau_1 \leqslant \tau \leqslant \tau_2$, has proved to be most effective, yielding the following relaxation function:

$$G(t, T) = 1 + \frac{1}{\ln \frac{\tau_2}{\tau_1}}\left[\mathrm{Ei}\left(-\frac{t}{\tau_2}\right) - \mathrm{Ei}\left(-\frac{t}{\tau_1}\right)\right], \tag{7}$$

where $\mathrm{Ei}\left(-\frac{t}{\tau_i}\right)$ denotes the so-called exponential integral [3, 4, 27–29]. Dependent on the width of the interval of relaxation times, as characterized by the limits $[\tau_1, \tau_2]$, the relaxation function (7) allows the approximation of a variety of different processes—from narrow Debye peaks, over moderately broadened maxima up to extended plateau-like relaxation zones [4, 28], cf section 1—by least squares filling the parameters (Q, ΔQ, τ_0 and amplitude) of individually contributing processes to the experimental data.

3. Results

3.1. Characteristics of the MAE spectra

For ease of argument, figure 1 shows the MAE spectra of perfectly stoichiometric magnetite of which, however, the tunnelling-induced lower wing (4 K $< T <$ 35 K) already after

Table 1. Compilation of the activation parameters of relevant processes contributing to the presently discussed MAE spectra in Ti(x)-doped magnetite, $0.1 \leqslant x \leqslant 1.0$. The data of evaluable processes are marked in the last column by the figure numbers under which the respective spectra are depicted; processes which in certain concentration ranges are Not EValuable are denoted by NEV; processes occurring only in *stoichiometric* Fe_3O_4 ($x = 0$)—adjoined here for the ease of comparison—are marked by NOB (Not OBserved) with references for further information. The various MAE processes occurring in magnetite-based compounds are—*historically*—classified as follows: (V) *electronic induction* due to incoherent tunnelling in form of extended plateau-like (V_{I1}) ($4\ K < T < 20\ K$) and localized Debye-Type (V_{I2}) relaxations (30 K); (V_{II}) variable range hopping ($50\ K < T < 125\ K$), here confined to an irregular ('negative') peak near 65 K (V_{IIi}); (IV) *ionic induction* near 200 K—associated with reorientating interstitials; (III) vacancy-mediated diffusion of (Fe) ions; (II) type-III like diffusion mode, however, higher activated due to impurity induced-interactions causing shiftings to $T \geqslant 340$ K; (I) further ionic diffusion-type relaxations occurring at elevated temperatures ($T > 550$ K).

Process	T (K)	x	Q (eV)	ΔQ (ev)	τ_0 (10^{-14} s)	Figure
V_{I1}	$4 < T < 20$	0.0	0.03	0.02	10 000	NOB
V_{I2}	30	0.0	0.075	0.01	100	[9, 10, 18]
V_{IIi}	$\simeq$65	0.1	0.23	0.03	0.0001	2a
		0.2	0.23	0.04	0.0001	2b
IV_1	$\simeq$200	0.1	0.54	0.08	90	2a
		0.2	0.54	0.12	240	2b
		0.3	0.51	0.13	138	3a
		0.5	0.64	0.14	8.6	3b
		0.6	—	—	—	NEV
IV_2	$\simeq$220	0.1	0.68	0.22	4.6	2a
		0.2	0.73	0.21	0.2	2b
		0.3	0.68	0.18	0.3	3a
		0.5	0.73	0.20	0.01	3b
		0.6	—	—	—	NEV
III_1	300_-	0.0	0.82	0.14	9.6	NOB
III_2	300_+	0.0	0.96	0.12	0.17	[8–10, 28]
III^*	260	0.1	0.68	0.21	4.7	2a
	>0.1	—	—	—	—	NEV
II_1	>360	0.1	—	—	—	NEV
		0.2	1.09	0.16	66	2b
		0.3	1.16	0.12	0.54	3a
		0.5	1.01	0.11	32	3b
		0.6	0.84	0.12	481	4a
II_2	>400	0.1	—	—	—	NEV
		0.2	1.24	0.15	76	2b
		0.3	1.39	0.12	0.64	3a
		0.5	1.19	0.25	20	3b
		0.6	0.95	0.10	1000	4a

minute Ti doping ($0.0001 \leqslant x \leqslant 0.008$) becomes severely affected and for $x \geqslant 0.05$ is completely suppressed [1–3, 8–12], cf figures 1 to 4. Accordingly, within the relatively high concentration range of our present experiments ($0.1 \leqslant x \leqslant 1.0$) this type of low-temperature relaxation is completely suppressed, cf section 1. On the other hand, the higher-temperature plateau ($50\ K < T < 125\ K$)—arising from variable-range small-polaron hopping, being activated above a temperature gap extending from $35\ K < T < 50\ K$ [3, 10, 28]—survives in strongly reduced and modified form up to Ti^{4+} contents of $x < 0.5$, cf figures 2(a)–3(b).

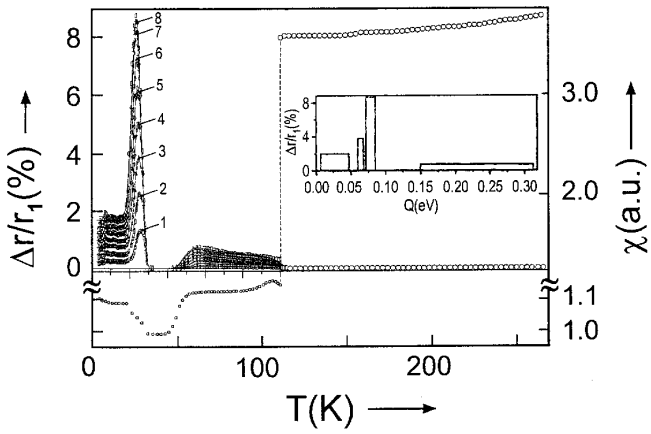

Figure 1. Typical MAE spectrum, together with initial susceptibility χ_0 (in arbitrary units (a.u.)), cf section 2.2—clearly indicating the Verwey transition by its spontaneous jump near 125 K—of perfectly stoichiometric, single crystalline Fe_3O_4. The various isochronals of the spectrum are characterized by the times t_1 and t_2, elapsed after sample demagnetization, i.e., $t_1 = 1$ s; (1) $t_2 = 2$, (2) 4, (3) 8, (4) 16, (5) 32, (6) 64, (7) 128, (8) 180 s (section 2.2). The inset shows the energy distributions of participating processes, as determined from numerical fitting (continuous lines) of the experimental data (symbols).

The corresponding perturbation of ionic order in these systems is also clearly reflected in the susceptibility curves of figures 2–4—as compared to the stoichiometric Fe_3O_4 standard (figure 1)—indicating only for $x = 0.1$ a strongly mutilated Verwey transition peak, shifted to $T_V < 100$ K (figure 2(a)), whereas for higher Ti contents (figures 2(b)–5(b)) the Verwey transition is completely suppressed [3].

Interestingly, after lower doping ($0.1 \leqslant x \leqslant 0.3$)—near the onset of small-polaron hopping (∼65 K)—a pronounced sign-reversed, negative MAE (V_i)[7], arises which—regarding structure and temperature position (figures 2(a)–3(a))—is unique so far, as compared to other related ferrite compounds, cf [3, 8–12], footnote 6.

The presence of B-site vacancies (δ) in the inverse spinel lattice is known to give rise to various relaxations in the temperature range near 300 K, as investigated previously in detail on a series of magnetite-based compounds, $Fe_{3-x}M_xO_{4+\delta}$, doped with different cations (M), all of which are referenced in [3, 10–12], cf footnote 6. Accordingly, the following vacancy-mediated relaxation processes may be expected in our experiments (cf section 4).

(i) The basic process III—associated with jumps of Fe^{2+} ions into neighbouring B-site vacancies, usually composed of two processes III_1 and III_2, centred at 300 K [8–11]. This process, however, is completely absent in the present spectra—in agreement with our former observations on corresponding *polycrystalline* $Fe_{3-x}Ti_xO_{4+\delta}$ compounds where this relaxation, too, was found to become already suppressed for doping rates of $x > 0.025$ [1, 2], as reported similarly by Schmidbauer *et al* from MAE studies on polycrystalline titanomagnetites [23].

(ii) The lower-temperature process III* (260 K)—a modified version of process III, occurring

[7] In terms of the systematic process classification in magnetite-based ferrites, mentioned in the table caption, this process should be denoted as V_{IIi}—'i' standing for 'irregular'. Since, however, in the present context of the family of group *V* processes only the 'negative' 65 K process is of relevance, we denote it henceforth by the abbreviated form V_i.

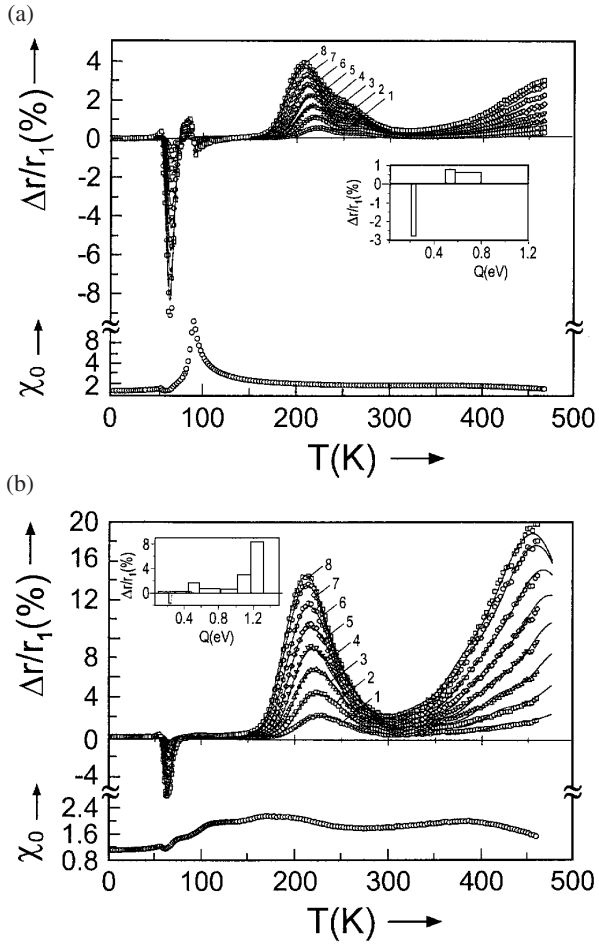

Figure 2. MAE spectrum and initial susceptibility of single crystalline $Fe_{3-x}Ti_xO_{4+\delta}$ ($\delta \simeq 0.005$, cf section 2.1) for (a) $x = 0.1$ and (b) $x = 0.2$; technical details as in figure 1.

typically only after *low-dose* Ti^{4+} ($x < 0.1$), [1, 2], and possibly higher-dose Mn^{2+} ($x > 0.3$) doping [11]. In the present concentration range of $x \geqslant 0.1$, however, this process plays only the role of a background relaxation, in agreement with previous observations on *polycrystalline* $Fe_{3-x}Ti_xO_{4+\delta}$ [1, 2, 23], cf figures 2–5.

(iii) Process II, known to occur after doping with any type of cation—in the simultaneous presence of B-site vacancies—as a typical high-temperature satellite ($T > 325$ K) of process III [3, 9–11]. As a unique feature in our present experiments we observe process II to become systematically shifted upon increased doping ($0.1 \leqslant x \leqslant 0.6$)—as indicated already in [23] —from *higher* to *lower* temperatures (480 K $> T >$ 380 K), cf figures 3–5, as compared to a usually reversed temperature variation in other related compounds, cf [1, 2, 9–11], cf footnote 6.

(iv) In addition, similarly as in Ti^{4+} doped *polycrystalline* Fe_3O_4 [1, 2], a pronounced relaxation occurs around 210 K (cf figures 2(a)–3(b)) which in previous investigations on related systems has been associated with reorientations of intrinsic interstitials [1, 2, 28], cf section 4.

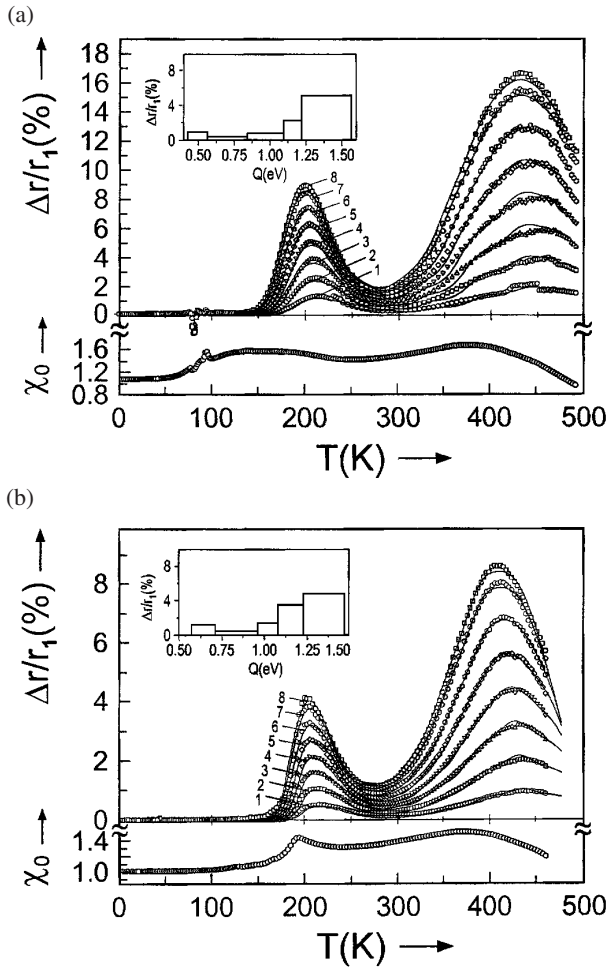

Figure 3. MAE spectrum and initial susceptibility of single crystalline $Fe_{3-x}Ti_xO_{4+\delta}$ ($\delta \simeq 0.005$, cf section 2.1) for (a) $x = 0.3$ and (b) $x = 0.5$; technical details as in figure 1.

3.2. Numerical analysis of the MAE spectra

Figures 2–4 give a survey of the effect of continued Ti^{4+} doping on the respective MAE spectra, using a presentation which combines the experimental data (symbols) with their numerical approximations (continuous lines, interconnecting the respective data points). The process parameters determined from these fittings, according to section 2.3, are summarized in table 1 and are found to be in reasonable agreement with the values of the corresponding relaxations determined previously on *polycrystalline* $Fe_{3-x}Ti_xO_{4+\delta}$ [1, 2]. Additionally, these MAE spectra are supplemented by their respective temperature-dependent initial susceptibility curves (χ_0, in arbitrary units) which, frequently, provide further details on specific items of the observed relaxation processes.

Figures 5(a), (b) show, respectively, the strengths and temperature positions of the major processes investigated as functions of the Ti^{4+} content. The interesting features of these relations are (i) the concomitant passing through a maximum of process II and IV—already

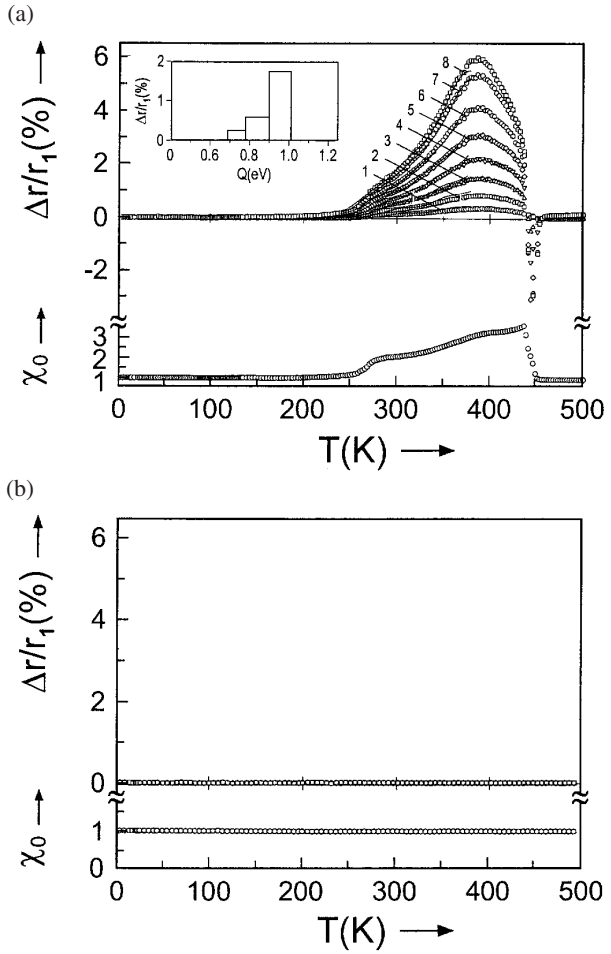

Figure 4. MAE spectrum and initial susceptibility of single crystalline $Fe_{3-x}Ti_xO_{4+\delta}$ ($\delta \simeq 0.005$, cf section 2.1) for (a) $x = 0.6$ and (b) $x = 1.0$; technical details as in figure 1.

observed for IV in our previous studies on *polycrystalline* Fe_3O_4 [1, 2] —(ii) the monotone decay of process V_i, within the present doping range (figure 5(a)) and (iii) the systematic, strong decrease of the maximum temperature of process II, in contrast to a moderately increasing T_{max} of process V_i and a relative constancy of process IV (figure 5(b)). These pronounced items will prove most valuable for an identification of the doping-induced relaxation processes, cf section 4.

4. Discussion

4.1. Electron-hopping induced relaxation processes—'negative' 65 K peak

As outlined in section 1, in the currently investigated doping range ($x \geqslant 0.1$), the low-temperature ($T \leqslant 35$ K) tunnelling processes are completely suppressed, whereas some modified form of variable-range small-polaron hopping persists in the temperature interval 50 K $< T <$ 125 K, for doping rates up to $x \leqslant 0.3$.

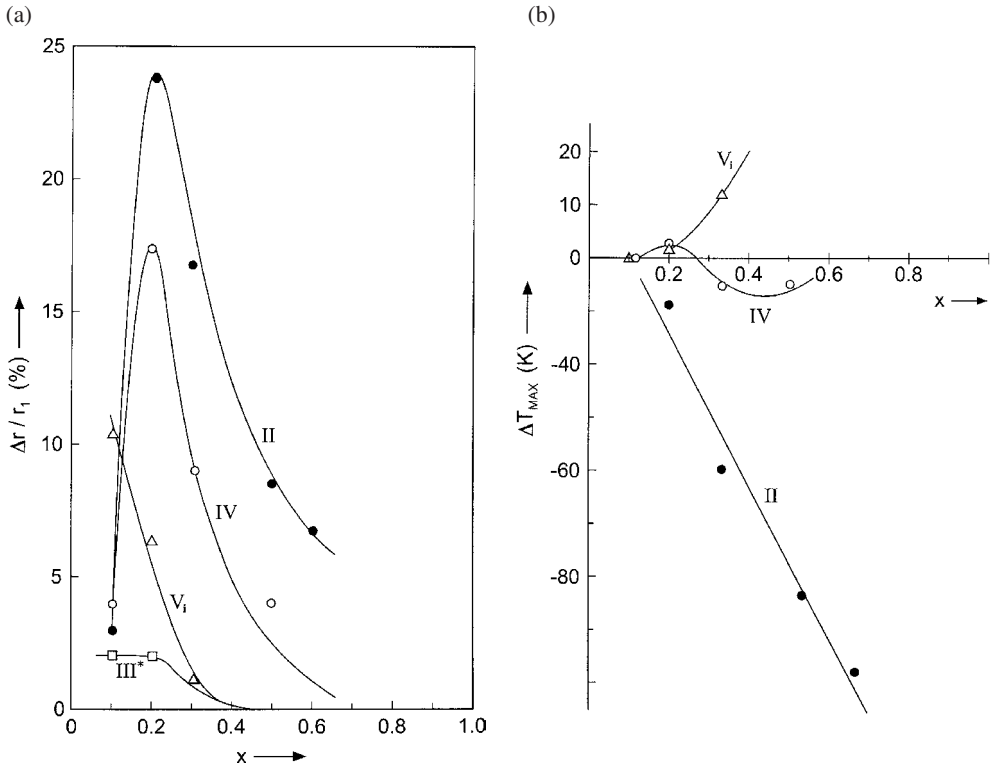

Figure 5. (a) Amplitudes of the dominant relaxation processes as functions of Ti doping, x. The maxima of processes II and IV indicate the transition from exclusive B-site substitution of Ti^{4+}-induced 'extra'-Fe^{2+} (for $x < 0.2$) to preferential A-site occupation. (b) Peak temperature shifting of prominent processes on continued Ti^{4+} doping. Pronounced, monotone variations (processes II and V_i) are associated with doping-enforced Coulomb interactions, in contrast to the less doping-dependent process IV, which is regarded to be rather of stress-induced origin.

The interesting feature of these residual hopping processes in the current *single crystalline*—as opposed to the previously investigated *polycrystalline* [1, 2]—Ti-doped magnetite consists of the fact that they occur here, evidently, as a superposition of two *counteracting* contributions giving rise to process V_i

(i) the usual standard hopping process, tending to form a plateau-like relaxation in the range of 50 K $< T <$ 125 K (cf section 3.1), and
(ii) a pronounced doping-dependent, *sign-reversed* ('negative') Debye-type MAE[8] near 65 K (cf figures 2(a)–3(b)), whose strength is found to become steadily diminished on increased doping ($x \geqslant 0.1$), cf figure 5(a).

It seems most appropriate to open the discussion of the present MAE spectra with this latter, negative disaccommodation process near 65 K which, due to its temperature position, is

[8] It must be noticed here that, due to the superposition of these counteracting processes to the effective relaxation, not all individual isochronals of the corresponding 65 K peak (V_i)—which, regarding its general shape, half-width etc, is clearly of Debye type—can be well fitted numerically. This fact is also reflected by the analytically determined, somewhat unrealistic process parameters, cf table 1, of $\tau_0 = 10^{-17}$ s and $Q = 0.23$ eV. The effective relaxation time τ corresponding to these parameters may be described mathematically equally well (cf equation (6))—and in better agreement with the corresponding data determined for other ferrite systems, [10, 11, 28] —by a more realistic combination of, e.g., $\tau_0 = 10^{-13}$ s and $Q = 0.18$ eV.

associated with modified electron hopping. The sign-reversal of this process is an indication of a corresponding relaxation-induced, time-dependent *increase* of the initial susceptibility—in contrast to its usually observed *decrease* during 'normal' MAEs, cf [3, 4, 10, 26, 27]. Since due to the Ti^{4+} zero-orbital groundstate, ($3d^0$:$^1S_0$), Ti-induced magnetocrystalline interactions may be excluded, we are led to associate this relaxation with an electron-supported mechanism of *local stress-release* between adjoining Fe ions, according to reaction (1). Indeed, considerable lattice distortions are expected to arise upon continued Ti doping since, by reason of charge neutrality, each implemented Ti^{4+}, besides replacing one Fe^{3+} ion, additionally causes one further Fe^{3+} to change its valency into an 'extra' Fe^{2+} ion, yielding as a final result a replacement of two Fe^{3+} ions by one Ti^{4+} and one Fe^{2+} ion.

Regarding the radii of the participating ions—being nearly coincident for Fe^{3+} (0.65 Å) and Ti^{4+} (0.61 Å), but considerably larger for Fe^{2+} ($\geqslant$0.75 Å), [30, 31][9] —it becomes evident that this process, producing a surplus of Fe^{2+} ions on B-sites, is connected with the introduction of internal stress into the spinel lattice. As a possible mechanism for local stress reduction we regard, as depicted in figure 6(a), electron hopping between neighbouring, alternatively Ti-resident and Ti-free B-type tetrahedra causing a stress reduction in the former tetrahedron—due to the replacement of one Fe^{2+} ion by an Fe^{3+} ion—as indicated in the following way[10]:

$$1\ Ti^{4+} + 3\ Fe^{2+} - e^- \quad \longrightarrow \quad 1\ Ti^{4+} + 1\ Fe^{3+} + 2\ Fe^{2+}. \tag{8}$$

The stress release thereby achieved in Ti^{4+} substituted tetrahedra—initiating a corresponding rise of the susceptibility—is regarded as the main source for the thermally activated 'negative' relaxation V_i near 65 K, cf figures 2(a), 3(a).

In this context, the distribution of the various ions over the A and B sites of the—initially inverse—spinel lattice is of great interest. Whereas the Ti^{4+} ions are generally agreed to be exclusively substituted on B sites [13, 21, 32], there exist various models concerning the sites being occupied by the excessively, Ti^{4+}-induced Fe^{2+} ions following (8): whereas Akimoto *et al* [33] assume a gradually increasing Fe^{2+} occupation of A sites departing from $x \geqslant 0$, Néel [34] and Chevallier [35] propose a corresponding A-site substitution to start only for $x \geqslant 0.5$, i.e., for Ti contents at which, on average, in all B-site tetrahedra just one Fe^{3+} ion is replaced by one Ti^{4+} ion (figure 6), cf section 4.2.4. An intermediate conception, deduced by O'Reilly and Bannerjee from electric conductivity measurements [36], assumes the onset of A-site occupation by Fe^{2+} ions for Ti^{4+} contents of $x \geqslant 0.2$. This model has been supported subsequently by extended conductivity [13, 21] and magnetization [16] studies. Moreover, Brabers [21] developed an analytical model, describing the Ti^{4+}-induced distribution of Fe^{2+} and Fe^{3+} on B and A sites, using—like Ihle and Lorenz [37, 38, 3]—a basic Hamiltonian including, besides the site energies E_A and E_B, only the near-neighbour Coulomb interaction U and a Fe^{2+}–Ti^{4+}-pair attraction energy, W [21]. In terms of realistic parameters—i.e., $U = 0.05$ eV; $W/U = -1$ and $E_A - E_B \geqslant 0.2$ eV—Brabers' model approaches the O'Reilly–Bannerjee occupation model.

The strength-dependence of the 'negative' 65 K MAE on Ti doping (figure 5(a)) is in agreement with a delayed substitution of extra Fe^{2+} ions on A sites—in the sense of the O'Reilly–Bannerjee and Brabers conceptions—since its pronounced amplitude at $x = 0.1$ (figure 2(a)) points to a still large number of Fe^{2+} ions residing on B sites and participating in the envisaged process of valency-mediated stress reduction. The respective amplitude decay

[9] In [30] the ionic radius of Fe^{2+} is given as 0.75 Å (Pauling) and 0.83 Å (Goldschmidt), whereas in [31] 0.78 Å is given as the most reliable value.

[10] This reaction has to be regarded as the result of two counteracting trends of the ferrite system: (i) to minimize its Coulomb energy, i.e. by obeying the Anderson rule of appointing $10/2e^+$ charges to each B-type tetrahedron and (ii) to minimize the substitution-induced magnetostrictive interaction energy. In proposing a system reaction according to (8), we argue in favour of a predominance of the latter (magnetostrictive) interaction in our present titanomagnetites.

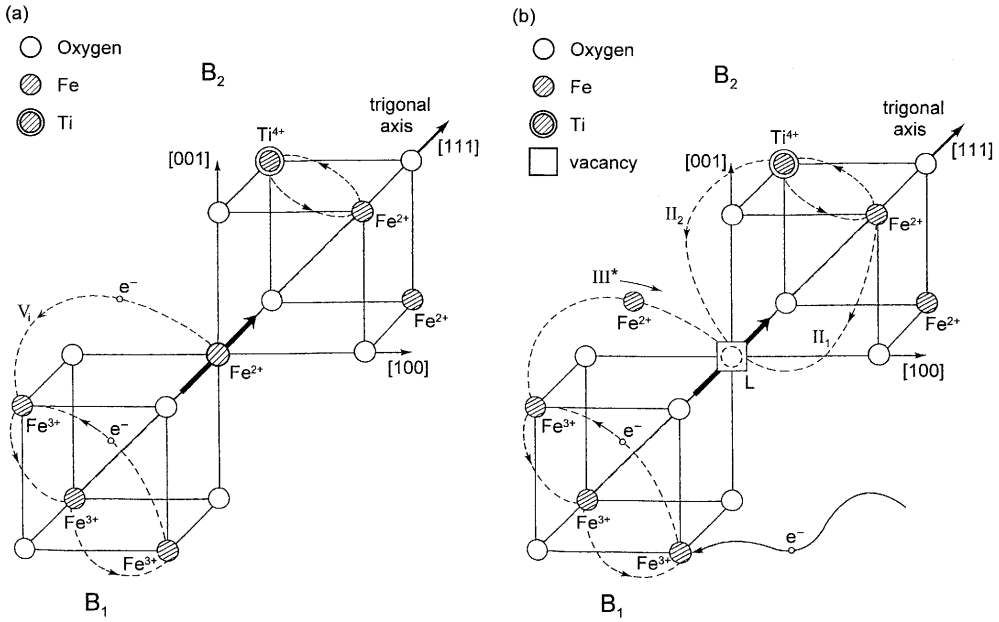

Figure 6. (a) Low-temperature electronic relaxations in Ti-doped magnetite: (i) process V_i, near 65 K, resulting from electron hopping out of the Ti^{4+} -lodging (B_2) into the Ti-free (B_1) cube—of the elementary B-site double-cube configuration—connected with stress release in B_2; (ii) additional low-temperature ($4\ K < T < 35\ K$) relaxation mechanisms—suppressed, however, in the present range of Ti doping—are feasible due to tunnelling-induced electron transfer, as indicated in B_1. (b) Ionically induced relaxations—at $T > T_V \simeq 125$ K, in the presence of Ti^{4+} ($0.1 \leqslant x \leqslant 1.0$) and B-site vacancies, L—are dominated by interactive stresses originating, i.e., from inherent ⟨111⟩ lattice distortions and anisotropic Fe^{2+}–Ti^{4+} pairs (cf B_2). Accordingly, the activation enthalpies for jumping of Fe^{2+}, $Q(II_1)$, and, possibly, Ti^{4+} ions, $Q(II_2)$, considerably exceed the value $Q(III)$ of Fe^{2+} jumping in undoped magnetite. On the other hand—due to a doping-induced relative electron surplus in the lattice—Fe^{2+} jumping between residual Ti-free cubes (B_1) gives rise to process III* with even reduced enthalpies, $Q(III^*) < Q(III)$.

on increased doping ($0.1 \leqslant x \leqslant 0.3$) is associated with an onset of A-site substitution of Fe^{2+} ions, causing both an inhibition of electron exchange and,—due to a decreasing number of Ti-free B-site cubes, cf figure 6(a)—a diminution of respective valency-mediated stress release.

4.2. Ionically induced relaxation processes

4.2.1. Process IV, near 210 K. MAEs, situated in the temperature range around 210 K—denoted usually as type-IV processes [10, 11] —have been previously observed in Fe_3O_4 *single crystals* following e^--irradiation [28] and in *polycrystals* after doping with Mn^{2+} [11], Ba^{2+} [39] and Ti^{4+} [1, 2].

The association of process IV with relaxing *interstitial*-type defects has been convincingly deduced from e^--irradiated stoichiometric Fe_3O_4 single crystals by systematically analysing the specific radiation-induced MAE spectra and their recovery upon stepwise annealing [28]. This interpretation was based on the following assumptions:

(i) similar defect production (i.e., intrinsic interstitials and vacancies) during low-temperature e^--irradiation in the inverse spinel lattice as in the well-studied cubic and hexagonal metal lattices [4, 28];

(ii) existence of considerable interstitial-induced lattice distortions, as indicated by the occurrence of a pronounced anomalous spike-like peak near the Verwey transition ($\simeq$125 K), which from previous high-temperature quenching of polycrystalline Fe_3O_4 has been identified as an extremely sensitive probe on internal stresses [7, 28, 39];

(iii) an intimate, stress-induced relationship between process IV and this spike-like peak, as supported by a synchronous annealing behaviour, ending in their annihilation at $T_a \geqslant 350$ K [28].

In previous experiments on cation-doped polycrystalline Fe_3O_4, the strongest process IV effect has been observed in higher-dose Ba^{2+}-doped magnetite, $Fe_{3-x}Ba_xO_{4+\delta}$ ($x \geqslant$ 1 at.%), [39]. There, too, this relaxation is accompanied by an anomalous spike-like peak near 100 K, similar to that in e^--irradiated magnetite. On account of this correspondence and in view of the considerably greater ionic radius of Ba^{2+} (1.4 Å) as compared to Fe^{3+} (0.64 Å) and Fe^{2+} (0.83 Å), [30, 31], these MAEs, too, were associated with intrinsic interstitials, there produced under the action of pronounced Ba^{2+}-induced lattice distortions [10, 39]. This same mechanism was also regarded to be responsible for the occurrence of process IV in Mn^{2+}-doped Fe_3O_4, though with minor strength, on account of lattice distortions arising from the replacement of smaller Fe^{3+} (0.64 Å) by somewhat larger Mn^{2+} (0.83 Å) ions [11]. In agreement with these preceding interpretations it appears reasonable to associate the actual process IV, too—like in recent investigations on polycrystalline $Fe_{3-x}Ti_xO_{4+\delta}$ [1, 2]—with thermally activated relaxations of intrinsic interstitial-type defects.

An interesting feature of our present experiments consists of the concomitant occurrence of the stress-induced process IV (210 K) together with the obviously related *negative* Debye-type peak (V_i) near 65 K. The absence of this negative peak in former investigations revealing, nevertheless, process IV—i.e. e^--irradiated stoichiometric *single-crystalline* Fe_3O_4 [28] or impurity-substituted (Ba^{2+} [39], Mn^{2+} [11], Ti^{4+} [1, 2]) *polycrystalline* magnetite—suggests an association of its occurrence with Jahn–Teller type *long-range* stress-ordering. Such long-range ordering—being suppressed in *polycrystals* due to an intergranular outbalancing of randomly oriented stress components—is supposed to preferentially occur in *single crystals*, at low enough impurity contents so as to keep type-(1) electron exchange still active. Evidently, in preceding experiments these preconditions were not satisfied, due to either lack of long-range stress-ordering (*polycrystals*) or predominance of lattice damaging (e^--irradiated *single crystals*), thus suppressing electron exchange according to (1) [3, 28].

Consequently, we regard the occurrence of this negative 65 K peak (V_i) in *single crystals* as the product of cooperative interactions between various sources of local anisotropy, such as (i) residual Fe^{2+} orbital moments, extra-stabilized on B-sites in form of tightly bound Fe^{2+}–Ti^{4+} pairs and (ii) Coulomb-induced, $\langle 111 \rangle$-directed inherent lattice distortions, being supported in the presence of B-site vacancies [1, 2], cf sections 4.2.2 and 4.2.3. Due to the order-induced superposition of these contributions, a large unidirectional overall—stress-evoking—anisotropy of Jahn–Teller type is established, preferentially in single crystals, which is regarded as the main source for the 65 K MAE.

4.2.2. Processes III and III.* These peaks have been fully described in our previous studies on polycrystalline Ti^{4+}-doped magnetite [1, 2], where they were found to occur only in low Ti-doped ($x \leqslant 0.025$) samples and to become strongly reduced on higher doping. In accordance with this previous finding, both processes are also suppressed in the concentration range of our present experiments—$x(Ti^{4+}) \geqslant 0.1$—we therefore summarize their items only to the extent necessary for a consistent interpretation of the present MAE spectra.

In numerous previous investigations the 300 K peak has been found to be a sensitive qualitative and quantitative [3, 8–11, 28, 39–41] indicator of the presence of octahedral vacancies in the inverse spinel lattice. Numerical analysis revealed this process to be composed of at least two Debye-type processes, III_1 and III_2 [8–11], resulting from reorientations of trigonally distorted octahedral B-site vacancies, following thermally activated jumping of anisotropic Fe^{2+} ions. Typically, these two processes differ by about the activation enthalpy of electron hopping ($Q_h \simeq 0.1$ eV) and consequently have been attributed to

(i) directly jumping Fe^{2+} (III_1, $Q \simeq 0.84$ eV), and
(ii) Fe^{2+} ions which, prior to jumping, had to be formed from Fe^{3+} ions by capturing an activated electron according to equation (2) (III_2, $Q \simeq 0.94$ eV) [1, 2, 8–11].

Process III* has been interpreted as a derivative of III_1 which—in the presence of a Ti^{4+}-induced relative abundance of Fe^{2+} ions and a correspondingly increased number of mobile electrons—results from Fe^{2+}-jumping with respectively reduced activation enthalpies of $Q_{III^*} \simeq 0.7$ eV [1, 2], cf figure 6(b).

4.2.3. Process II. As pointed out in section 3.1, this relaxation occurs typically in single- and polycrystalline magnetite after any type of cation doping [3, 9–11, 39] as a high-temperature shoulder of process III ($T_{II} \geqslant 360$ K). Upon continued doping it is usually shifted to higher temperatures—as typically observed, for instance, in Mn-doped polycrystals [11]. Another example of extremely pronounced shifting has been observed previously in Ti^{4+}-doped polycrystalline Fe_3O_4, i.e. from $T_{II} \simeq 400$ K to $T_{II} \geqslant 480$ K by varying $x(Ti^{4+})$ within the narrow range of $0.01 \leqslant x \leqslant 0.025$ [1, 2, 23]. In agreement with this finding in polycrystalline Fe_3O_4, we observe in our relatively strongly Ti-doped single crystals ($x \geqslant 0.1$) process II to be located, already for $x = 0.1$, at about $T_{II} \geqslant 480$ K. Here, however, with increasing x this process becomes shifted to lower temperatures, thus ending, e.g., for $x = 0.6$ at $T_{II} \simeq 380$ K (figure 5(b)), cf [23].

In our previous studies on polycrystalline magnetite [2], process II has been assigned to tightly bound Ti^{4+}–Fe^{2+} pairs out of which—after their thermally activated break off—Fe^{2+} ions are inducing this relaxation by jumping into neighbouring B-site vacancies[11], thereby causing a reorientation of their local anisotropy, cf section 4.2.2. In terms of this model, evidently, the activation enthalpy of process II may be regarded as the sum of the enthalpies for free Fe^{2+}-ion jumping (according to process III) and the respective Ti^{4+}–Fe^{2+} pair-binding. By comparing the activation data of processes II and III (table 1), this pair-binding enthalpy may be guessed to lie within the realistic range of $0.15 < H_B < 0.5$ eV, being compatible with respective results obtained from electric conductivity measurements [2, 21]. Interestingly, the highest stability of these complexes—corresponding to their maximum relaxation temperature of $T_{II} \geqslant 480$ K, cf figures 2(a), (b) and 5—occurs within the doping range ($0.1 \leqslant x \leqslant 0.2$) for which, from the strength of the 'negative 65 K process', also the maximum of Ti^{4+}-induced lattice distortions—and hence maximum number of intrinsic interstitials—is expected in the crystal, cf sections 4.1, 4.2.4. This interpretation compares well with our former argument (section 4.2.1) that—preferentially in single crystalline compounds—Jahn–Teller-like, cooperative, long-range interactions between dopant-induced lattice distortions and anisotropic Fe^{2+}–Ti^{4+} pairs lead to a stabilization of these pairs, as manifested in a considerable increase of their binding enthalpies.

[11] In [2] we have discussed in detail the alternative possibility that—instead of the Fe^{2+} ion—the Ti^{4+} ion may jump into the vacancy and thereby contribute as well, by a variation of the local anisotropy, to an additional, modified magnetic relaxation. In terms of this argument the enormous width of process II may be explained as the superposition of two related processes [1, 2], cf table 1.

4.2.4. Dose-dependence of relevant processes. The variations of amplitudes and temperature-positions of the observed processes with Ti concentration (figures 5(a), (b)) provide us with further valuable information on finer details of the respective relaxation mechanisms. Thus, a striking feature in figure 5(a) is the parallel, steep ascent of processes II and IV, culminating in a maximum near $x = 0.2$, which is followed by a moderate decrease approaching zero for $x \geqslant 0.7$. Remarkably, this maximum is close to $x = 0.25$, i.e. the concentration at which all potential vacancy sites, L, interconnecting two elementary B-site cubes (cf figure 6(b)) are expected to be decorated by just one Ti^{4+} ion[12]. At this Ti content the various processes may be affected as follows:

(i) Concerning process II, this concentration is distinguished by the greatest possible number of single $Fe^{2+}Ti^{4+}$ pairs residing near a vacancy—thereby forming a specific, substitution-induced modification of the original type-III configuration (figure 6(b)), cf section 4.2.3. The amplitude reduction of process II upon doping above this critical level is in agreement with the onset of Fe^{2+} redistribution on A sites. Moreover, the amplitude decay for $x > 0.25$ points to a reduction of the established long-range stress order in the crystal due to Coulomb repulsions between an increasing number of Ti^{4+} ions residing in adjacent B sited cubes (cf figure 6(b)). This lowering of long-range stress causes, additionally, a loosening of the $Fe^{2+}Ti^{4+}$ pair binding and hence a reduction of the activation enthalpy for ionic jumping out of this configuration which, in turn, leads to the pronounced low-temperature shifting of process II, cf figure 5(b).

(ii) The dependence of process IV on the Ti content may be explained in terms of the same arguments: on continued doping, due to the Ti^{4+}-induced lattice distortions, an increasing number of Fe^{2+} ions is expected to become displaced from their B-site positions. As thoroughly discussed in [2], the so-formed interstitials—under the action of the imposed long-range stress field—are stimulated to undergo reorientation-type relaxations which are identified to result from a superposition of at least two related processes, cf table 1. The occurrence of a strength-maximum for these processes, at a Ti content of about $x \simeq 0.2$ (figure 5(a)), is regarded again as an indication for the start of A-site substitution of 'extra' Fe^{2+} ions. For Ti contents $x > 0.2$, amplitude reductions are expected due to the described Ti-dependent diminution of the imposed crystalline stress field. In agreement with experiments (figure 5(a)), this relaxation type is expected to vanish at a doping rate of about $x \simeq 0.8$, i.e., the level at which the sum of atomic volumes in adjacent B-sited cubes (figure 6(a)) is the same[13] for both the Ti-substituted ($xTi^{4+} + (4 - x)Fe^{2+}$; $x > 1$) and the undoped case ($2Fe^{2+} + 2Fe^{3+}$). The relatively small peak temperature variation of process IV on Ti doping, x, as compared to process II (figure 5(b)), points to a relaxation resulting—instead of valency-dependent Coulomb-attractions—rather from stress-induced magnetostrictive lattice interactions, thus supporting the proposed view in terms of interstitial relaxations.

(iii) The steady amplitude decrease of the 65 K relaxation (V_i), starting from $x \geqslant 0.1$ (figure 5(a)), reflects the delicate interplay between the various interactions contributing to its formation: (a) internal stresses, originating from Ti^{4+}-induced anisotropic 'extra' Fe^{2+} ions (section 4.1) which, however, may be dislocated by means of (b) thermally

[12] Since Ti^{4+} is supposed to be exclusively substituted on B sites, a Ti content of $x = 1$ (corresponding to $Fe^{2+}_A[Fe^{2+}Ti^{4+}]_BO_4$, i.e. so-called ulvöspinel or ulvit) is equivalent to, respectively, 8 Ti ions on 16 B sites so that for $x = 0.25$ the basic, bi-cubic configuration of figure 6 contains just 1 Ti ion on its B sites.

[13] The vanishing of the Ti^{4+}-induced extra stress in a B-sited cube of figure 6 results from the following balance between the potential atomic volumina, Ω: $(1 + x^*) \cdot \Omega(Ti^{4+}) + (3 - x^*) \cdot \Omega(Fe^{2+}) = 2 \cdot \Omega(Fe^{2+}) + 2 \cdot \Omega(Fe^{3+})$. Using the atomic radii of footnote 7 and being aware of the relevant Ti content: $x = 0.25 + x^*$ (cf section 4.2.4), the concentration corresponding to a vanishing extra distortion yields $x \geqslant 0.8$.

activated electron hopping according to (1). Evidently, on increased Ti substitution ($x \geqslant 0.1$), the diminution of electron exchange outweighs all feasible process-supporting contributions—such as a rising number of potential relaxators (up to $x \leqslant 0.25$). Thus, as a net result of various influences, the steady strength reduction of figure 5(a) is obtained, so that a potential maximum of this process V_i—if existent at all—may be searched for at doping rates of $x < 0.1$. The monotone increase of the peak temperature with increasing x (up to $x \leqslant 0.3$, cf figure 5(b)) points, in contrast to process IV, to an electronically determined source of this relaxation—as proposed, i.e., in the form of the electron exchange mechanism (1)—which, via Coulomb interactions, reacts most sensibly on the presence of charge carrying lattice defects, such as substituted Ti^{4+} ions.

(iv) On increasing doping, when finally attaining with $x = 1$ the composition $Fe_2Ti_1O_4$—known as ulvöspinel or ulvit—no further changes of the susceptibility with time or temperature are observed, cf figure 4(b). This is exactly the result to be expected from the *normal* spinel lattice of $Fe_2Ti_1O_4$ with, for example, all Fe^{2+} ions substituted on tetrahedral A sites so that, evidently, none of the described MAEs—resulting from reactions of B-sited Fe^{2+} ions—are conceivable any longer. Moreover, the magnetic structure of this compound, below the Curie temperature near 120 K, is known to be antiferromagnetic, with a faint, canting-induced admixture of ferrimagnetism [42].

5. Conclusions

(1) Our investigations show that all MAEs occurring in $Ti^{4+}(x)$-doped, $0.1 \leqslant x \leqslant 1.0$, magnetite are dominated by substitution-induced lattice distortions in the octahedral (B) sublattice, arising from transformation of Fe^{3+} into Fe^{2+} ions of higher volume. The prominence of respective spectra in well-crystallized, single-phase *monocrystals*—as compared to *polycrystalline* specimens—points to an overwhelming regime of Jahn–Teller type, long-range stress fields established under the action of crystallographic order by a cooperative alignment of various locally evoked distortions.

(2) These internal stresses, by interaction with the combined charge-/anisotropy-transfer of carriers, evoke specifically modified relaxation mechanisms giving rise to modified MAE spectra: (i) transmutation of variable range small-polaron hopping into a stress-releasing process, giving rise to a pronounced 'negative' Debye peak near 65 K (process V_i); (ii) stress-induced expulsion of B-sited Fe ions into interstitial positions, where they contribute by thermally activated reorientation to the relaxation near 210 K (process IV); (iii) increase in Fe^{2+}–Ti^{4+} pair-binding to an amount so as to suppress the original type-III, vacancy-mediated, ionic diffusion in favour of an extremely high-temperature shifted (>480 K) satellite-process II.

(3) The unanimous strength dependence of process II and IV on Ti(x)-doping, besides revealing stress induction as the common source of their amplitude-modulation, marks—by the coincidence of their maxima near $x \simeq 0.2$—a change in the substitution mode of 'extra' Fe^{2+} ions. Upon further doping to $x > 0.2$, Fe^{2+} ions are preferentially dissolved on tetrahedral A sites, thus leading to a stress release within the octahedral sublattice. These conclusions, concerning the substitution of Ti-induced 'extra' Fe^{2+} ions, compare well with previous arguments on results obtained by alternative techniques [16, 21, 36].

(4) A different nature of processes V_i and II, on the one hand, and process IV, on the other hand, is deduced from the nonconforming dependence of their peak temperatures on continued Ti doping: whereas peaks V_i and II, on increasing x, become drastically shifted—though in opposite directions: i.e., $T_{P,II}$ to lower and $T_{P,Vi}$ to higher temperatures—peak IV remains rather unaffected. This behaviour suggests a separation of the observed relaxations

into (a) valency-affected, Coulomb-type processes, such as '*diffusion*' combined with local *anisotropy-transport* of (i) small polarons (process V_i) and (ii) bivalent B-site vacancies (process II), and (b) *reorientation* of intrinsic interstitials (process IV), following rather magnetostrictive, stress-induced interactions.

References

[1] Torres L, Walz F, Bendimya K, De Francisco C and Kronmüller H 1997 *Phys. Status Solidi* a **161** 289
[2] Walz F, Torres L, Bendimya K, De Francisco C and Kronmüller H 1997 *Phys. Status Solidi* a **164** 805
[3] Walz F 2002 *J. Phys.: Condens. Matter* **14** R285
[4] Blythe H J, Kronmüller H, Seeger A and Walz F 2000 *Phys. Status Solidi* a **181** 233
[5] Walz F 1977 *Phys. Status Solidi* a **40** 455
[6] Walz F, Weidner M and Kronmüller H 1980 *Phys. Status Solidi* a **59** 171
[7] Kronmüller H and Walz F 1980 *Phil. Mag.* B **42** 433
[8] Kronmüller H, Schützenauer R and Walz F 1974 *Phys. Status Solidi* a **24** 487
[9] Walz F, Brabers V A M, Chikazumi S, Kronmüller H and Rigo M O 1982 *Phys. Status Solidi* b **110** 471
[10] Walz F, Brabers V A M and Kronmüller H 1997 *J. Physique Coll.* **7** C1 569
[11] Walz F, Rivas J, Brabers J H V J and Kronmüller H 1999 *Phys. Status Solidi* a **173** 467
Walz F and Rivas J 1976 *Phys. Status Solidi* a **37** 151
[12] Walz F, Brabers J H V J and Brabers V A M 2002 *Z. Metallk.* **93** 1095
[13] Kuipers A J M and Brabers V A M 1979 *Phys. Rev.* B **20** 594
[14] Kozlowski A, Rasmussen R J, Sabol J E, Metcalf P and Honig J M 1993 *Phys. Rev.* B **48** 2057
[15] Kozlowski A, Kakol Z, Kim D, Zalecki R and Honig J M 1996 *Phys. Rev.* B **54** 12093
[16] Kakol Z, Sabol J and Honig J M 1991 *Phys. Rev.* B **44** 2198
[17] Knowles J E and Rankin P 1971 *J. Physique Coll.* **32** (Suppl 2–3) C1 845
[18] Knowles J E 1974 *Philips Res. Rep.* **29** 93
[19] Brabers V A M 1995 *Handbook of Magnetic Materials* vol 8, ed K H J Buschow (Amsterdam: Elsevier) pp 189–324
[20] Honig J M 1995 *J. Alloys Compounds* **229** 24
[21] Brabers V A M 1995 *Physica* B **205** 143
[22] Höhne R, Melzer K, Hochschild H, Libor G and Krause R 1975 *Phys. Status Solidi* a **27** K117
[23] Schmidbauer E and Fassbinder J 1987 *J. Magn. Magn. Mater.* **68** 83
[24] Bendimya K, De Francesco C, Hernandez P, Alejos O and Munoz J M 1997 *J. Physique Coll.* **7** C1 605
[25] Brabers V A M, Whall T E and Knapen P S A 1984 *J. Cryst. Growth* **69** 101
[26] Walz F 1971 *Phys. Status Solidi* a **8** 125
Walz F 1974 *Appl. Phys.* **3** 313
Walz F 1984 *Phys. Status Solidi* a **82** 179
Walz F 1995 *Phys. Status Solidi* a **147** 237
[27] Kronmüller H 1968 *Nachwirkung in Ferromagnetika* (Berlin: Springer)
[28] Walz F and Kronmüller H 1990 *Phys. Status Solidi* b **160** 661
Walz F and Kronmüller H 1994 *Phys. Status Solidi* b **181** 485
[29] Jahnke-Emde-Lösch 1966 *Tafeln Höherer Funktionen* (Stuttgart: Teubner)
[30] *Gmelins Handbuch der Anorganischen Chemie* 1929 vol 59 (Weinheim: Verlag Chemie GmbH)
[31] Shannon R D 1976 *Acta Crystallogr.* A **32** 751
[32] Wechsler B A, Lindsley D H and Prewitt C T 1984 *Am. Mineral.* **69** 754
[33] Akimoto S, Katsura T and Yoshida M 1957 *J. Geomagn. Geoelectr.* **9** 165
[34] Néel L 1955 *Adv. Phys.* **4** 191
[35] Chevallier R, Bolfa J and Matthieu S 1955 *Bull. Soc. Fr. Minéral. Cristallogr.* **78** 307
[36] O'Reilly W and Banerjee S K 1965 *Phys. Lett.* **17** 237
[37] Lorenz B and Ihle D 1975 *Phys. Status Solidi* b **69** 451
[38] Ihle D and Lorenz B 1980 *Phil. Mag.* **42** 337
[39] Walz F, Rivas J, Martinez D and Kronmüller H 1994 *Phys. Status Solidi* a **144** 177
Walz F, Rivas J, Martinez D and Kronmüller H 1994 *Phys. Status Solidi* a **143** 137
[40] Walz F and Kronmüller H 1991 *Phil. Mag.* **64** 623
[41] Brabers V A M, Walz F and Kronmüller H 1998 *Phys. Rev.* B **58** 14163
[42] Akimoto S I 1964 *J. Phys. Soc. Japan* **17** (Suppl B–I) 706